

Article

Identification of Degradation Products of the New Anticancer Drug Substance ONC201 by Liquid Chromatography–High-Resolution Multistage Mass Spectrometry

Maxime Annereau ^{1,2} , Marina Vignes ^{1,2}, Tahar Sif Eddine Bouchema ¹, Lucas Denis ², Audrey Solgadi ³, Victoire Vieillard ⁴, Muriel Paul ^{4,5}, André Rieutord ² , Jacques Grill ^{6,7}, Philippe-Henri Secretan ^{1,*} , and Bernard Do ^{1,4,*}

¹ Matériaux et Santé, Université Paris-Saclay, 91400 Orsay, France

² Clinical Pharmacy Department, Gustave Roussy Cancer Campus, 114 rue Edouard Vaillant, 94800 Villejuif, France

³ CNRS, Ingénierie et Plateformes au Service de l'Innovation Thérapeutique, Université Paris-Saclay, Inserm, 91400 Orsay, France

⁴ Department of Pharmacy, Henri Mondor Hospital, AP-HP, 94000 Créteil, France

⁵ EpidermE, Université Paris Est Creteil, 94010 Creteil, France

⁶ Molecular Predictors and New Targets in Oncology, INSERM, Gustave Roussy, Université Paris-Saclay, 94800 Villejuif, France

⁷ Département de Cancérologie de l'Enfant et de l'Adolescent, Gustave Roussy, Université Paris-Saclay, 94800 Villejuif, France

* Correspondence: philippe-henri.secretan@universite-paris-saclay.fr (P.-H.S.); bernard.do@aphp.fr (B.D.)



Citation: Annereau, M.; Vignes, M.; Bouchema, T.S.E.; Denis, L.; Solgadi, A.; Vieillard, V.; Paul, M.; Rieutord, A.; Grill, J.; Secretan, P.-H.; et al. Identification of Degradation Products of the New Anticancer Drug Substance ONC201 by Liquid Chromatography–High-Resolution Multistage Mass Spectrometry. *Chemosensors* **2023**, *11*, 294. <https://doi.org/10.3390/chemosensors11050294>

Academic Editor: Cláudia Maria Rosa Ribeiro

Received: 3 April 2023

Revised: 10 May 2023

Accepted: 12 May 2023

Published: 15 May 2023



Copyright: © 2023 by the authors. Licensee MDPI, Basel, Switzerland. This article is an open access article distributed under the terms and conditions of the Creative Commons Attribution (CC BY) license (<https://creativecommons.org/licenses/by/4.0/>).

Abstract: ONC201 (dordaviprone) is a new drug substance used in a compassionate manner to treat patients with glioblastoma. Given the clinical context and the particularly promising preclinical results, we have been asked by the medical authorities to make a first treatment available throughout France as a hospital preparation to allow access to treatment and to conduct clinical trials. However, to control the quality and safety conditions inherent in this academic manufacturing process, while there is virtually no data available to date to understand the stability of ONC201, we had to determine the stability profile of ONC201, i.e., its sensitivity to different stressors and the types of impurities that could form during its degradation. We found that ONC201 was sensitive to oxidation in the presence of hydrogen peroxide or under light irradiation. Both conditions resulted in the formation of 20 degradation products detected and identified by liquid chromatography–high-resolution mass spectrometry. Their structural elucidation required an in-depth study of the fragmentation pattern of protonated ONC201, described for the first time. The product ions of the degradation products were compared to those of ONC201 protonated ion to assign the most plausible structures for all the detected degradation products. Of these degradation products, those that were rapidly produced, of high intensity and/or identified as potentially having a different toxicity profile to ONC201 by in silico studies, were selected to be monitored during batch release testing and stability studies.

Keywords: ONC201; dordaviprone; degradation products; LC-MS²; MS fragmentation patterns; structural elucidation; oxidation; control specifications; in silico

1. Introduction

ONC201 (7-benzyl-4-(2-methylbenzyl)-1,2,6,7,8,9-hexahydroimidazo [1,2-a]pyrido [3,4-e]pyrimidin-5(1H)-one) is a medication currently investigated in clinical trials for the treatment of children with diffuse intrinsic pontine gliomas (DIPG) associated with the histone H3 K27M mutation [1,2] as well as for the treatment of other solid tumours [3,4]. It is the first member of a novel class of anti-cancer small molecules named imipridones [5]

and exerts several mechanisms of action including a p53-independent inducer of the death ligand TRAIL gene transcription and stress induction [6]. Currently, it is a non-labelled drug in Europe and Gustave Roussy Cancer Centre is the only one in France to produce dosage forms comprising ONC201.

Since the end of 2021, the hospital pharmacy manufactures the treatment for a secured compassionate access in France and Europe. This manufacturing could continue in the open-label, controlled trial evaluating the efficacy of ONC201 versus everolimus, called BIOMEDE 2.0 [7]. As this is a new active substance for which there are very few data, it was necessary in this clinical context to properly characterise the compound physico-chemically to establish a knowledge base essential to pharmaceutical development and the design of a strategy control adapted to the quality risks. The need to develop such knowledge is supported by the existence of recent similar research works on drug substances of other pharmacological classes such as antiretrovirals [8–10] and tyrosine kinase inhibitors [11–13], where the authors often rely on mass spectrometry-based analysis to determine the structures of their degradation products. Currently, no research article is available on the degradation products of ONC201 as well as that of the other imipridones.

In this article, part of this work pertaining to ONC201 is reported. It concerns analytical work to better understand the intrinsic stability of ONC201, by highlighting (i) the main parameters to which this new substance is sensitive and (ii) the potential degradation products likely to be formed in situations of non-control of quality of the drug.

On a practical level, we have already had the experience of such work [14,15] and were inspired both by similar studies [11,16] and by the recommendations of the ICH [17]. As we are in a predictive approach, there was no other way to work on degradation products than to have generated them by exposing ONC201 to various stress conditions, on condition of applying them in such a way as to have a certain predictive value [18,19].

The structural approach aimed at identifying the degradation products in a sufficiently informative manner was based on the use of liquid chromatography–mass spectrometry coupling to mass spectrometry set in high-resolution- and multi-stage mode [20]. The use of other orthogonal methods was not carried out, but the richness and the precision of information obtained by this approach made it possible to access structural information sufficiently supported to go further in the search for information aimed at establishing provisory specifications for release control and stability control as part of BIOMEDE 2.0 [7].

2. Materials and Methods

2.1. Reagents

ONC201 dihydrochloride (DiHCl) (batch #S22S02C27; purity > 99%) was purchased from MedKoo Biosciences (Morrisville, New York, NY, USA). Analytical grade acetonitrile came from Sigma-Aldrich (St Quentin-Fallavier, France). Ultrapure water was produced by the Direct-Q[®] 3 UV system (Merck, Guyanourt, France). Hydrogen peroxide (H₂O₂) 30% *v/v* was supplied by Carlo Erba SDS (Val de Reuil, France), whereas hydrochloric acid and sodium hydroxide were obtained from Sigma-Aldrich (St Quentin-Fallavier, France).

2.2. Analytical Conditions

Analytical conditions were developed using a non-targeted approach, by resorting to reverse phase chromatography in gradient mode.

Chromatographic analyses were carried out on UltiMate 3000 HPLC system (Les Ulis, France) coupled to a diode array detection and an Orbitrap[™] mass spectrometer. Phenomenex C18 column (250 × 4.6 mm; 5 μm) represents the stationary phase and was maintained at 30 °C for the duration of the analysis. A total of 20 μL samples were injected. The wavelength of the UV detection was 220 nm. The flow rate was 1 mL·min⁻¹. The following gradient mode was applied: 0–2 min: 95% A; 2–30 min: 95 → 0% A; 30–35 min: 5 → 95% A, where A consists of 0.1% (*v/v*) formic acid in pure water and B consists of 0.1% (*v/v*) formic acid in acetonitrile. MS, MS² (MS-HRMS) and MS³ (MS-HRMS²) mass spectra were acquired by using an Orbitrap[™] Q Exactive[™] Plus detector (Thermo Fisher

Scientific, Waltham, MA, USA). The MS data were processed using Xcalibur® software (version 2.2 SP 1.48).

2.3. Forced Degradation Test

Forced degradation studies were performed in accordance with ICH Q1A (R2) [17] and Q1B [21] guidelines. Stress studies on ONC201 were performed under photolytic, oxidative, hydrolytic and thermal conditions. The hydrolytic (acidic and basic), photolytic and oxidative stress studies were performed in solution phase, while the thermal stress was performed in solid phase.

For thermal stress, ONC201 powder was stored in an oven at 105 °C for 15 days. The impact of acidic and basic stress was studied by diluting a stock solution at 5 mg·mL⁻¹ (ONC201 dihydrochloride), in equal parts with hydrochloric acid 1M and sodium hydroxide 1M, respectively. The samples were stored at 40 °C and were analysed every day for one week. The oxidation of ONC201 was studied by preparing an aqueous solution containing 3% H₂O₂ and 2.5 mg·mL⁻¹ of ONC201 dihydrochloride. This solution was stored at room temperature and the samples were analysed after 0, 30, 60, 90, 120, 180 and 240 min of exposure.

For photodegradation studies, experiments were conducted by exposing an aqueous solution of ONC201 dihydrochloride (2.5 mg·mL⁻¹) to simulated light, and samples were collected at 60 min, 3 h, 6 h, 24 h and 48 h. A light beam with a wavelength range of 300–800 nm was emitted from Q-SUN Xe-1 xenon lamp (Q-Lab Corporation, Saarbrücken, Germany) with window mode operation, according to ICH Q1B. The intensity was 1.50 W·m⁻² at 450 nm.

2.4. In Silico Toxicological Assessment

Following the guidance of ICH M7 [22], two computational approaches have been used with the view to assess the mutagenic potential of all identified degradation products. The two software consisted of Toxtree [23], a rule-based system, and T.E.S.T. [24], a quantitative structure-activity relationships (QSAR)-based system. For the QSAR-based system, the consensus method was chosen because according to EPA's user guide for T.E.S.T., it was shown to achieve the best prediction results during external validation.

3. Results and Discussion

Schematically, this work first involves an observational study based on monitoring the behaviour of ONC201 under different stress conditions (Section 3.1). The degradation products detected in majority according to a selection criterion based on thresholds defined by the related ICH guidelines were then analysed structurally by high-resolution mass spectrometry in multi-stage mode (Section 3.2). Based on the tentatively established structures, toxicity studies using an in silico approach were carried out (Section 3.3) with a view, ultimately, to select the degradation impurities to be monitored in the context of stability studies of finished products for the determination of shelf life.

3.1. Stability Profile of ONC201 Based on Its Behaviour under Different Stress Conditions

The input data considered to frame this study are the following:

- The guidelines ICH Q3A [25] and ICH Q3B [26] have proposed thresholds beyond which specific measures (reporting, identification and toxicological qualification) must be undertaken for the degradation products. In the precise case of ONC201, as the intake of ONC201 may not exceed 100 mg per day, the thresholds of identification applicable for the drug substance and for the drug product, calculated from peak areas in LC-UV, are 0.1% and 0.2%, respectively. Thus, it was decided that any degradation product for which the signal exceeded 0.1% relative to that obtained for ONC201 should be identified.
- In addition, to avoid considering irrelevant degradation products, none of the products formed after loss of more than 20% of ONC201 were studied, as they are considered

unlikely to occur under real storage conditions. The aim was indeed to obtain as much predictive value as possible from these results.

- ONC201 was found to be stable under hydrolytic and thermal stress conditions, as no degradation products were detected.

By opposition, in a photolytic or oxidising environment, we observed that the molecule is quickly degraded (see Supplementary Materials, Figure S1). When analysing solutions obtained under conditions leading to a loss of about 15% of ONC201, 13 and 8 degradation products under photolytic and oxidative conditions required identification, respectively. All the degradation products detected under HPLC-UV were also highlighted by mass spectrometry detection. Typical HPLC-MS chromatograms are shown in Figure 1.

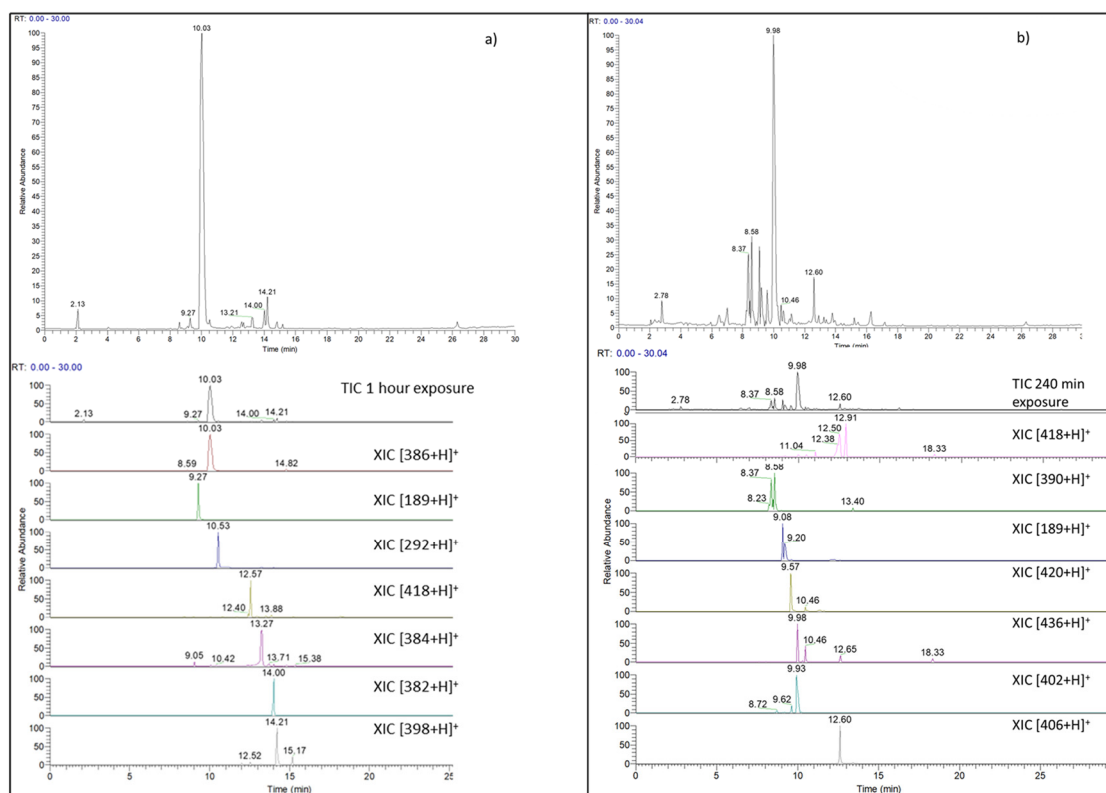


Figure 1. (a) Total and extracted chromatogram of aqueous ONC201 after 60 min of exposure to photolytic conditions; (b) total and extracted chromatogram of aqueous ONC201 after 240 min of exposure to oxidative conditions.

3.2. Structural Elucidation of the Main Degradation Products

3.2.1. High-Resolution Mass Spectrometry Studies

An essential prerequisite for the structural elucidation of ONC201 degradation products was to fully understand the process of drug fragmentation. Indeed, assuming that the compounds formed from ONC201 under stress conditions are structurally related to it, the differences observed in their respective mass spectra have enabled us in most cases to establish the structural change and thus to propose structures consistent with the fragmentation data.

Having so far found no information in the literature on how the protonated ONC201 ion fragments within the orbitrap under the analytical conditions used, we present below a detailed interpretation of its mass spectrum acquired in MS² (Figure S2) mode based on the acceptable differences between the exact and accurate masses to validate our hypotheses. From now on, it is important to note that the m/z values in the spectra correspond to

accurate mass values, whereas those we show in the fragmentation figures are theoretical or exact mass values.

3.2.2. Protonated ONC201 Fragmentation Pattern

According to its mass spectrum, MS² fragmentation of protonated ONC201 (Figure 2 inset (A), molecular formula = C₂₄H₂₇N₄O⁺, double bond equivalent, DBE = 13) gave rise to the formation of three intense daughter ions, the accurate masses of which (m/z 268.145, m/z 164.082 and 105.070) are respectively consistent with the following elemental formulas: C₁₆H₁₈N₃O⁺, C₈H₁₀N₃O⁺ and C₈H₉⁺. The mass spectrum also includes three other less intense ions, characterised by m/z 283.155, m/z 120.081 and m/z 91.054, to which correspond formulas C₁₆H₁₉N₄O⁺, C₈H₁₀N⁺ and C₇H₇⁺, respectively.

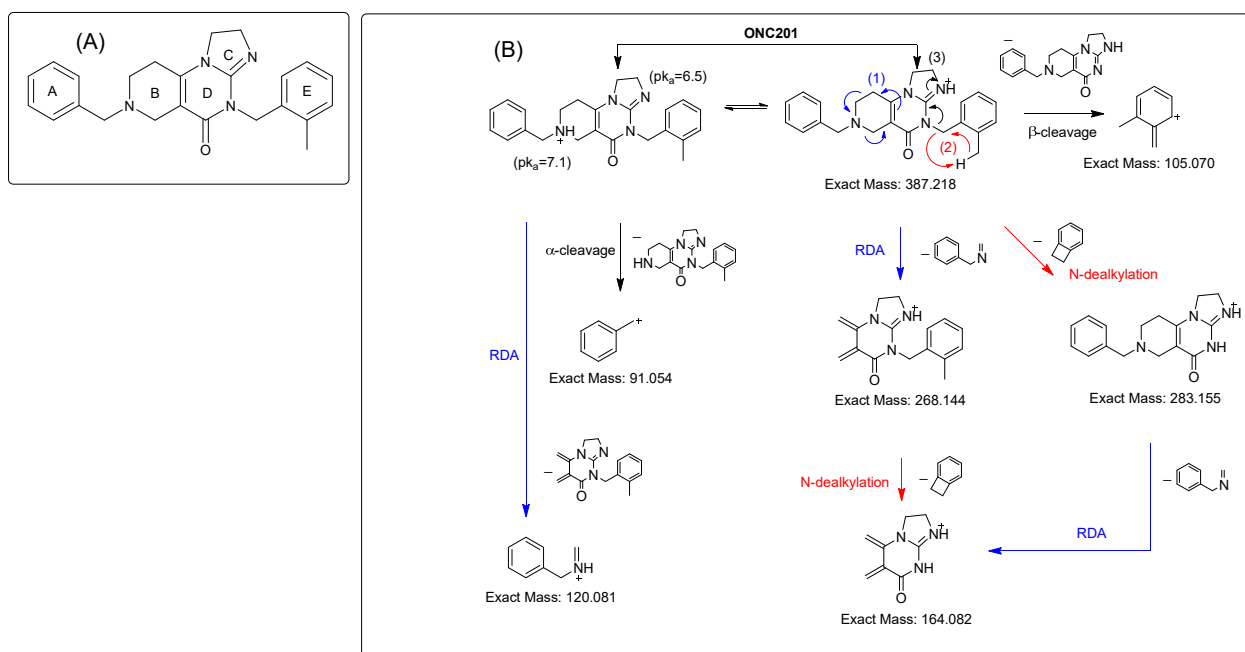


Figure 2. (A) Structure of ONC201 and naming of characteristic groups; (B) fragmentation pattern of protonated ONC201.

Particularly in the present case, it appeared that the formation of these product ions was closely linked to where protonation took place. ONC201 exhibits two basic functions, namely the imine function of the imidazole ring (pK_a = 6.5) and the tertiary amine of the piperidine group (pK_a = 7.1) (Figure 2).

After protonation of the amine function of ONC201, the molecular ion underwent α-cleavage to give the m/z 91.054 ion or retro Diels Alder rearrangement [27,28] (RDA) to give the ion m/z 120.081 ion (Figure 2, inset (B)).

Three other fragmentation pathways were highlighted, but these could only be explained by protonation of the imidazole-imine function. The most predominant is that involving RDA to give the m/z 268.144 ion which was responsible for the base peak. The next pathway, related to the presence of the m/z 105.070 ion, relies on a β-cleavage process due to a charge shift mediated by the iminium group. The third pathway involves the neutral loss of xylene, in all likelihood due to N-dealkylation. RDA and N-dealkylation are alternative processes that also apply to the product ions so that they in turn fragment. Indeed, after being formed by N-dealkylation, the m/z 283.155 ion underwent an RDA to form the m/z 164.082 ion, and conversely, the m/z 268.144 ion which was obtained by RDA would yield the 164.082 ion by N-dealkylation.

From this fragmentation study, we used the following information to help identify the structures of the degradation products:

- Any absence of neutral loss of the group at 119.073 Da by the RDA is an indicator that modifications have taken place on (i) the benzyl-tetrahydropyridine radical (A and B), (ii) the radical tetrahydropyridine (B), and/or (iii) the toluene radical (A) of ONC201 (Figure 2).
- Any absence of the neutral loss associated with the elimination of the group at 104.063 Da means that changes have occurred on the xylene radical of ONC201 (E).
- If these two neutral losses are present, on the other hand, we further explored the mass spectra data, in order to determine how modifications have taken place on the imidazole group (C) and/or the piperidinone group (D).

3.2.3. Proposed Structures of Degradation Products Resulting from Photolytic Stress

From here, the degradation products that will be identified by mass spectrometry will be systematically designated by “DPn”, where “DP” stands for “degradation product” and “n” is the nominal mass of the DP’s neutral form.

The descriptive data in Table 1 show, except for DP384, DP386 and DP418, that the degradation products formed and detected under photolytic conditions have two additional unsaturations compared to the ONC201 molecule. The DP384 and DP418 have only one extra and the DP386 has no extra. DP386 is merely an ONC201’s conformer and already described in the literature [29]. All spectral data are gathered in the Supplementary Materials.

Table 1. Accurate mass, best plausible formula, double bond equivalent and specific features detected under HRMS² conditions of the degradation products resulting from photolytic stress.

Accurate Mass (Name)	Best Plausible Molecular Formula	Number of Double Bond or Rings Equivalent	Presence of Daughter Ion or Neutral Loss Characteristic of		
			Retro Diels Alder (RDA)	O-xylene	Benzyl
387.216 (ONC201)	C ₂₄ H ₂₇ N ₄ O ⁺	13	Yes	Yes	Yes
190.133 (DP189)	C ₁₁ H ₁₆ N ₃ ⁺	5.5	No	Yes	No
293.140 (DP292)	C ₁₇ H ₁₇ N ₄ O ⁺	11.5	No	Yes	No
383.186 (DP382-1)	C ₂₄ H ₂₃ N ₄ O ⁺	15	No	Yes	Yes
383.186 (DP382-2)	C ₂₄ H ₂₃ N ₄ O ⁺	15	No	Yes	No
383.186 (DP382-3)	C ₂₄ H ₂₃ N ₄ O ⁺	15	No	Yes	No
385.202 (DP384-1)	C ₂₄ H ₂₅ N ₄ O ⁺	14	Yes	Yes	Yes
385.202 (DP384-2)	C ₂₄ H ₂₅ N ₄ O ⁺	14	No	No	Yes
387.216 (ONC201 isomer)	C ₂₄ H ₂₇ N ₄ O ⁺	13	Yes	Yes	Yes
399.181 (DP398-1)	C ₂₄ H ₂₃ N ₄ O ₂ ⁺	15	No	Yes	Yes
399.181 (DP398-2)	C ₂₄ H ₂₃ N ₄ O ₂ ⁺	15	No	Yes	No
399.181 (DP398-3)	C ₂₄ H ₂₃ N ₄ O ₂ ⁺	15	No	Yes	No
419.200 (DP418-1)	C ₂₄ H ₂₆ N ₄ O ₃ ⁺	14	Yes	Yes	Yes
419.200 (DP418-2)	C ₂₄ H ₂₆ N ₄ O ₃ ⁺	14	No	No	Yes

Apart from these observations, all the products continue to bear the xylene unit insofar as their mass spectra reveal the presence of neutral losses equal to 104.06 Da (Supplementary Materials). On the other hand, the transitions resulting from the loss of the group of 119.073 Da, attributed to the RDA, were only found for DP384 and 418 (Supplementary Materials).

These data allowed us to hypothesise that the degradation products presented in Table 1 were all at least oxidised at the dihydroimidazole moiety.

After further investigation of the mass spectrum of protonated DP384 and DP418, it was found that in contrast to all the phenomena described so far and those observed for the other degradation products formed under photolytic conditions, protonated DP384 and protonated DP418 lost imine and formimidic acid, respectively, during their fragmentation (transition m/z 385->m/z 356 and transition m/z 419->374, respectively). Although these are not the base peaks, the m/z 356 and m/z 374 ions both have high relative intensities, showing that the corresponding signals are not artefacts. However, such a departure could not be compatible with the configuration in which the tetrahy-

dropyridine amine is a tertiary amine, i.e., linked to the toluene group. Therefore, we hypothesised that the signal at m/z 385 and that at m/z 419 would in fact correspond to a mixture of conformers (isobaric products) with the same elemental composition but whose structures differ specifically at the tetrahydropyridine-toluene unit. It should be noted that source-induced production has been ruled out as this phenomenon has not been observed for ONC201. Under the action of light, abstraction of α -hydrogen can be expected when the tetrahydropyridine amine is not protonated. The formation of a radical site would lead to radical rearrangements resulting in the formation of two other conformers (Figure 3A). From this mixture of products of the same mass, as shown in Figure 3, each product ion in the spectra could be fully justified and explained (Figure 3B). As a result, DP384-1, DP384-2, DP418-1 and DP418-2 could be 7-benzyl-4-(2-methylbenzyl)-6,7,8,9-tetrahydroimidazo [1,2-a]pyrido [3,4-e]pyrimidin-5(4H)-one,14-(2-methylbenzyl)-5,6,8,8a,12a,12b-hexahydroimidazo [2''1'':2',3']pyrimido [5',4':3,4]pyrido [2,1-a]isoindol-13(14H)-one,7-benzyl-8-hydroxy-4-(2-methylbenzyl)-3a,4,6,7,8,9-hexahydroimidazo [1,2-a]pyrido [3,4-e]pyrimidine-2,5(1H,3H)-dione and 6-hydroxy-14-(2-methylbenzyl)-5,6,8,8a,12a,12b,14,14a-octahydroimidazo [2'',1'':2',3']pyrimido [5',4':3,4]pyrido [2,1-a]isoindole-2,13(1H,3H)-dione, respectively. It is likely that the LC-separative method used is not sufficiently resolving to separate these conformers, but analysis of the respective mass spectra did not conclude the singularity of each of the corresponding chromatographic peaks (RT 12.6 min and RT 13.3 min).

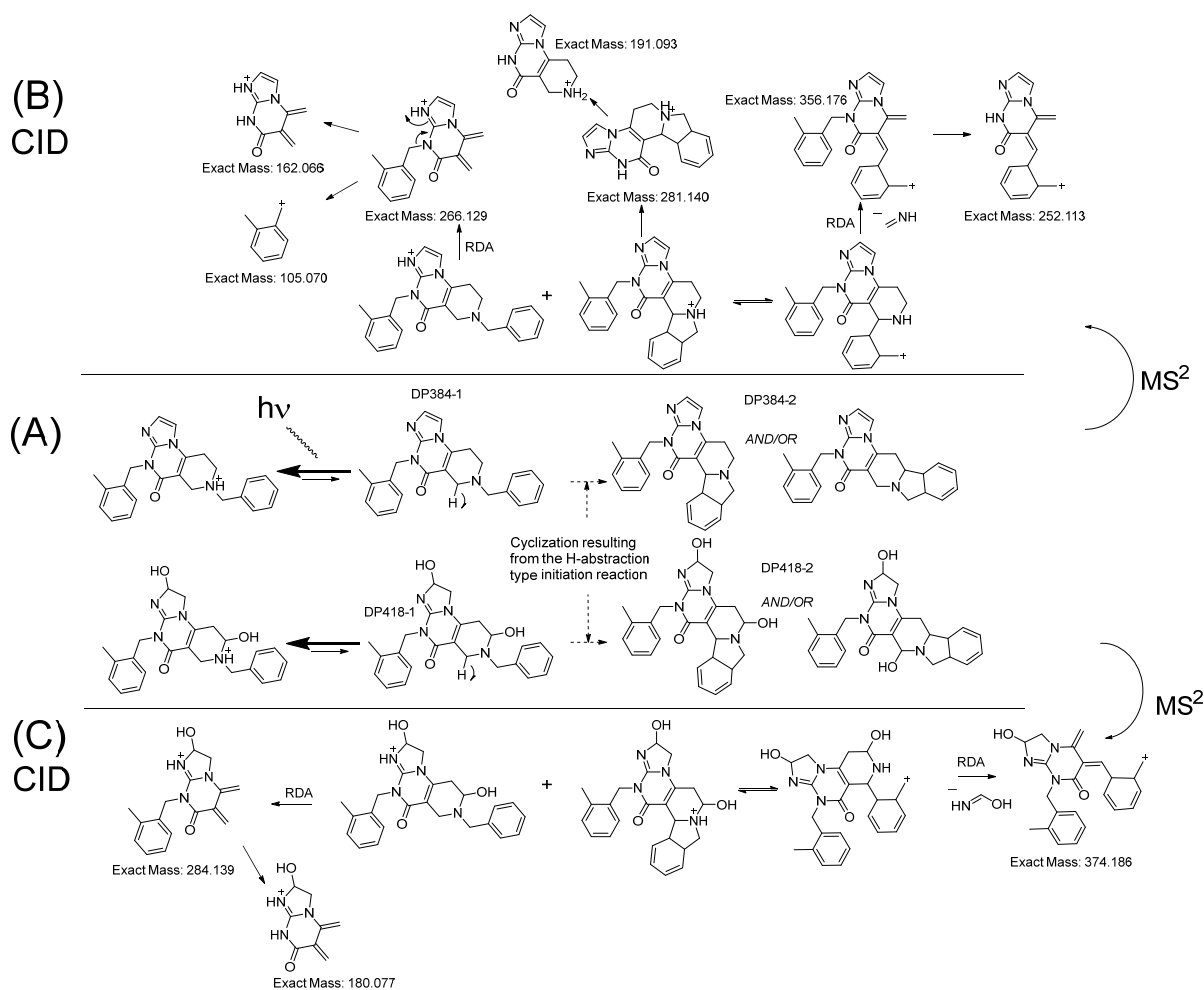


Figure 3. (A) Proposed mechanism related to light exposure leading to the formation of degradation products characterised by m/z 385 and m/z 419; (B) proposed fragmentation pattern of the m/z 385 ions; (C) proposed fragmentation pattern of the m/z 419 ions.

The formation of these degradation products confirmed that the imidazole group was considerably involved in ONC201 photodegradation, in line with what has been previously described for imidazole [30] as well as other drugs carrying the same group [31,32].

As mentioned above, the other products formed under photolytic conditions contain an extra double bond with respect to DP384 (Table 1). In all cases, this double bond was attributed to the transformation of the tetrahydropyridine moiety into the dihydropyridine moiety, which correlates with the absence of fragmentations resulting from RDA.

While it was straightforward to identify DP292 (Figure 4), which had simply lost the ONC201's toluene moiety under the action of light, the interpretation of the mass spectra related to protonated DP382 and DP398 necessitated the consideration of a mixture of isobaric products (conformers) to successfully explain the formation of the intense product ions in the mass spectra.

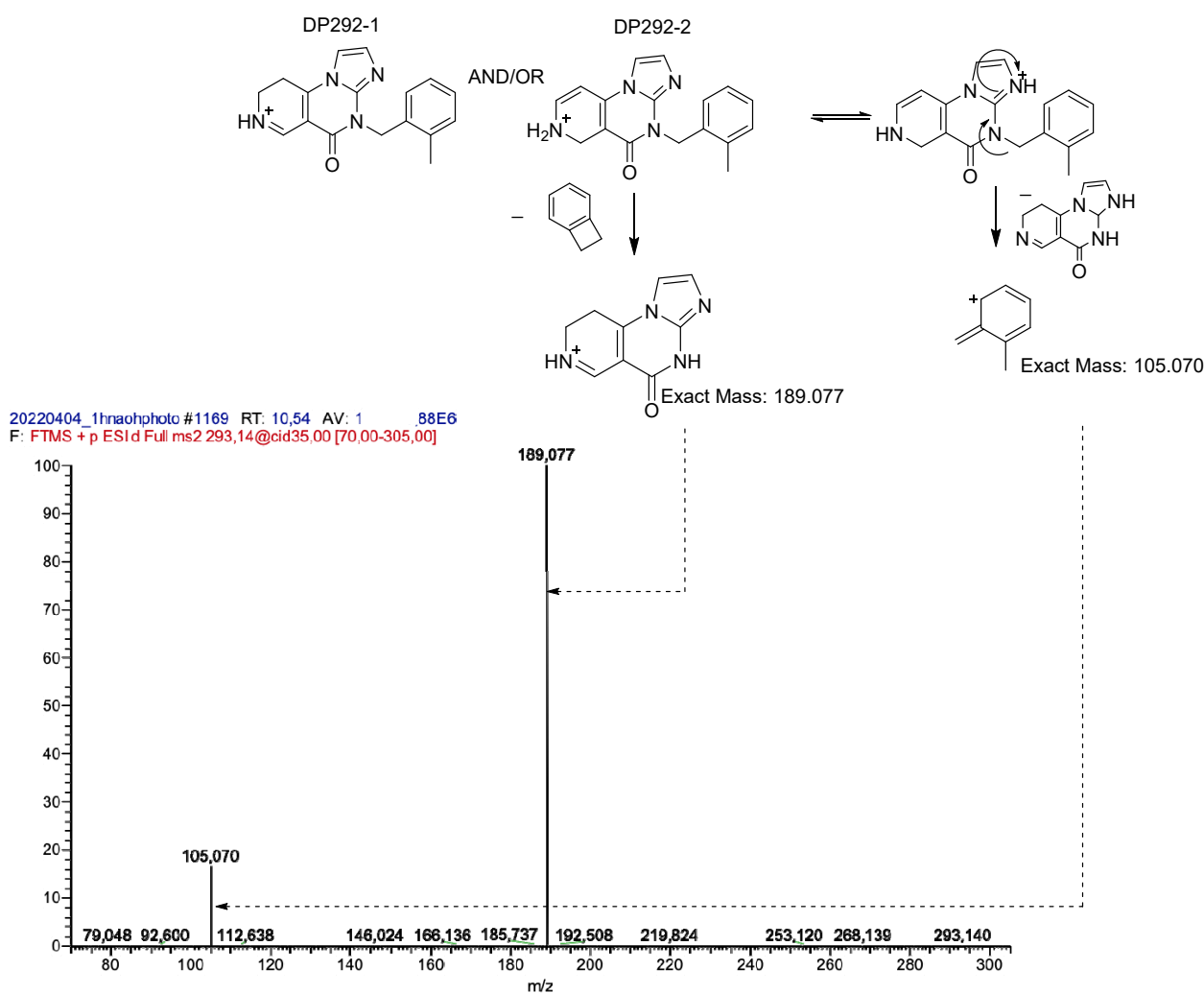


Figure 4. Proposed structures for DP292 and fragmentation pattern.

The fragmentation study of the molecular ions at m/z 383 and 399 shows very high similarities between them, i.e., (i) the same intense neutral losses, i.e., m/z 383- \rightarrow m/z 279 and m/z 383- \rightarrow m/z 189 for protonated DP383, compared to m/z 399- \rightarrow m/z 295 and m/z 399- \rightarrow m/z 205 for protonated DP399, and (ii) the presence in both of an intense product ion at m/z 195 (Supplementary Materials). The first-mentioned neutral loss is due to the departure of xylene, while the second-mentioned is related to that of a fraction of 194-Da. In terms of elemental composition, only one hydrogen atom and a positive charge differ between the 194-Da moiety and the m/z 195 ion. Indeed, this elemental composition

is consistent with that resulting from a moiety combining the xylene and toluene parts. However, given the spatial configuration of the ONC201 structure, it was not possible to imagine intra-molecular interactions leading to this type of grouping formed by covalent bonds under the action of light. Nor was it conceivable that such combinations could have taken place in the ESI source. In ESI source, combinations have been described for other molecules, but all referred only to the intervention of non-covalent interactions [33,34].

This is why, to explain the formation of these chemical groups under the action of light, we have put forward the hypothesis of intermolecular interactions because of radical α -cleavage and radical substitution (Figures 5A and 6A). From these reactions, it was possible to consider several co-eluted and isobaric structures as shown in Figures 5A and 6A. From this mixture of products of the same mass, as shown in Figures 5B and 6B, each product ion in the spectra could be fully justified and explained. As a result, DP382-1, DP382-2, DP398-1 and DP398-2 could be 7-benzyl-4-(2-methylbenzyl)-6,7-dihydroimidazo [1,2-a]pyrido [3,4-e]pyrimidin-5(4H)-one, 4-(2-methylbenzyl)-8,9-dihydroimidazo [1,2-a]pyrido [3,4-e]pyrimidin-5(4H)-one, 7-benzyl-4-(2-methylbenzyl)-6,7-dihydroimidazo [1,2-a]pyrido [3,4-e]pyrimidine-2,5(1H,4H)-dione and 4-(2-methylbenzyl)-8,9-dihydroimidazo [1,2-a]pyrido [3,4-e]pyrimidine-2,5(1H,4H)-dione, respectively. As indicated above, it is likely that the LC-separative method used is not sufficiently resolving to separate these conformers, but analysis of the respective mass spectra did not conclude the singularity of each of the corresponding chromatographic peaks (RT 14.0 min and RT 14.2 min).

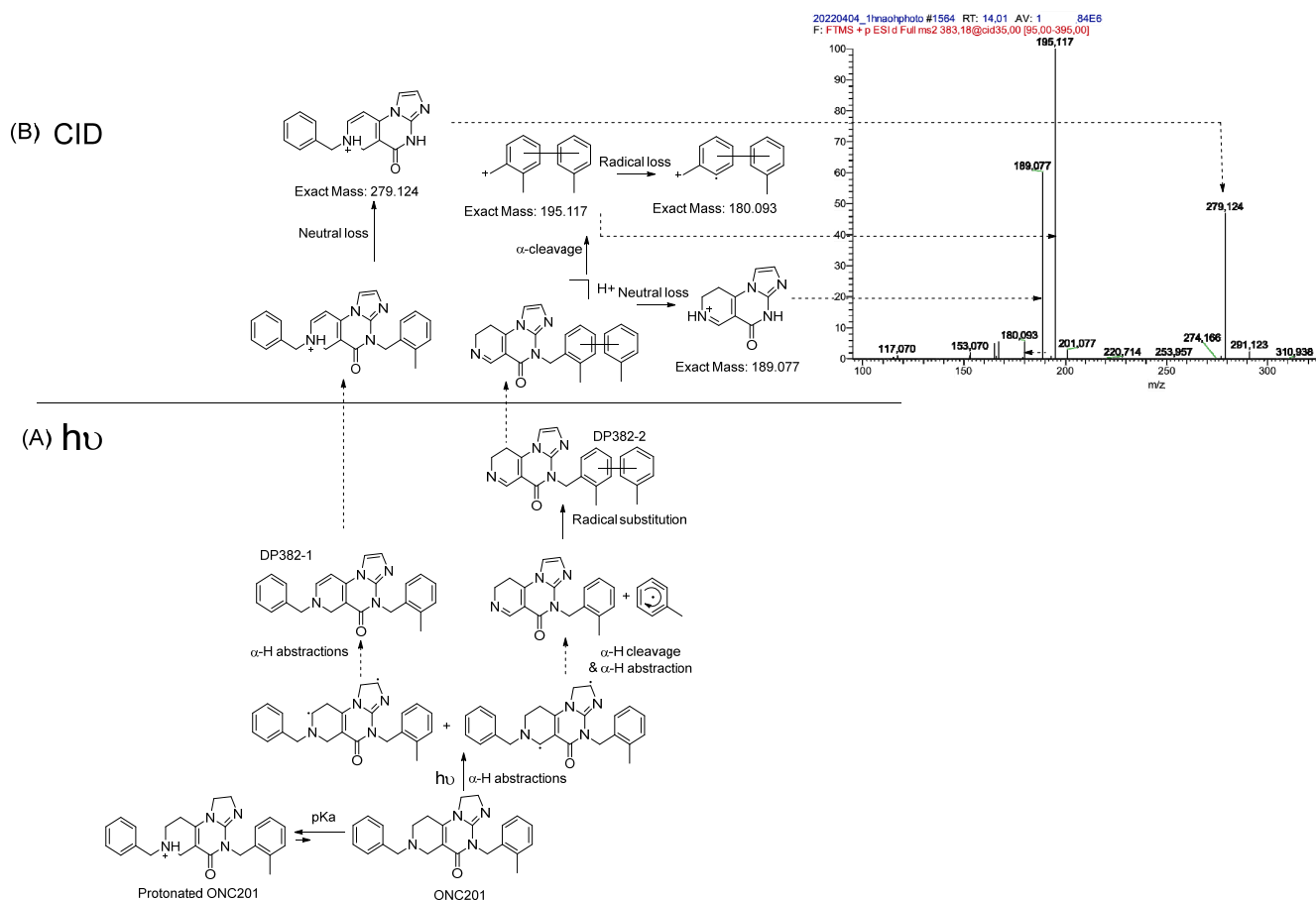


Figure 5. (A) Proposed formation pathways and structures of DP382s; (B) proposed fragmentation pattern of the m/z 383 ions.

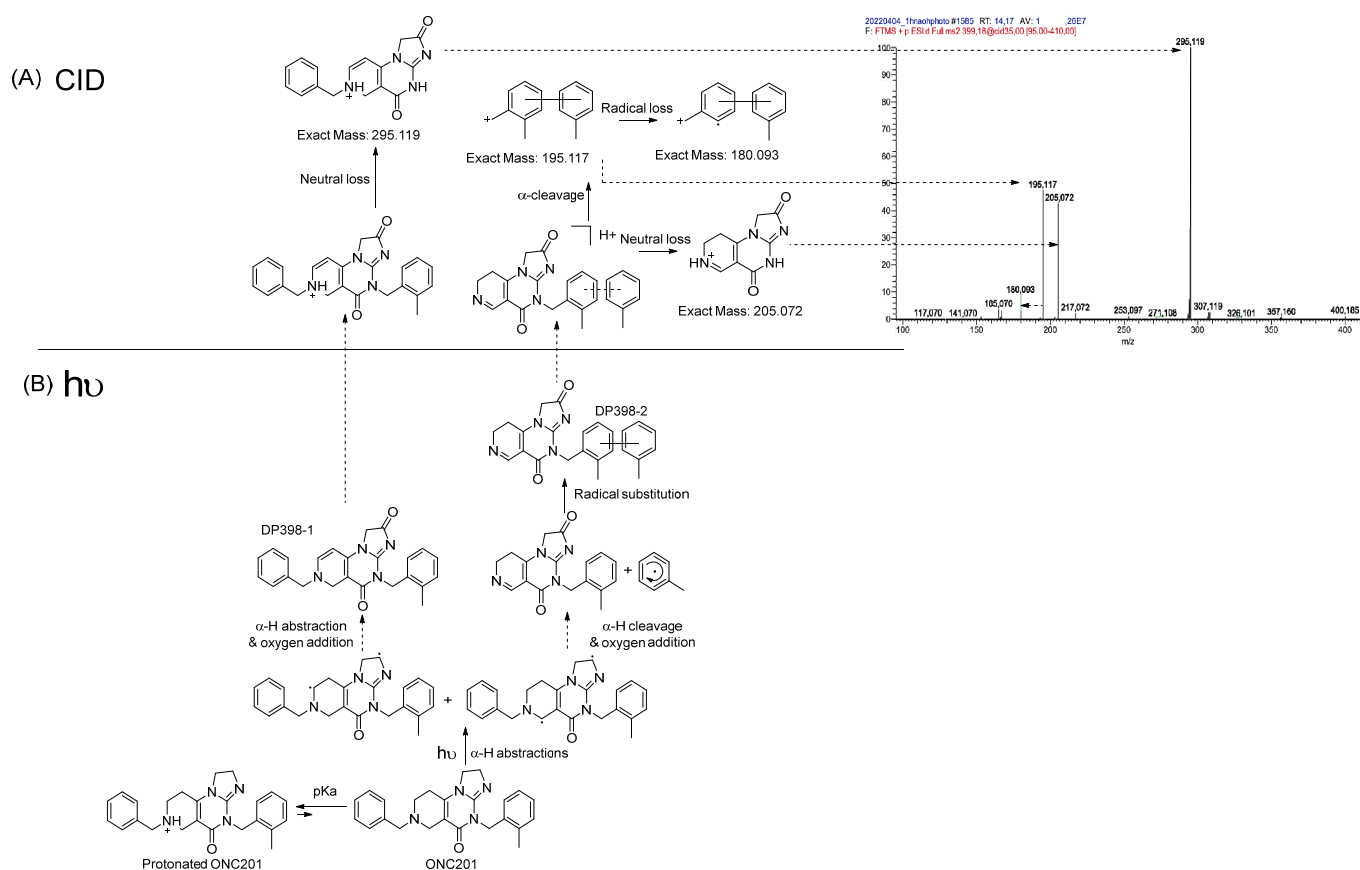


Figure 6. (A) Proposed formation pathways and structures of DP398s; (B) proposed fragmentation pattern of the m/z 399 ion.

3.2.4. Structural Elucidation of Degradation Formed under Oxidative Condition

In contrast to most degradation products from photolytic reactions, those formed in the presence of hydrogen peroxide have a higher mass than ONC201, except for DP189. Their elemental compositions, which are grouped in Table 2, show unambiguously, apart from DP189, that they all have a higher number of oxygen atoms than ONC201.

Table 2. Accurate mass, best plausible formula, double bond equivalent and specific features detected under HRMS² conditions of the degradation products formed under oxidative condition.

Accurate Mass (Name)	Best Plausible Molecular Formula	Number of Double Bond or Rings Equivalent	Presence of Daughter Ion or Neutral Loss Characteristic Of	
			Retro Diels Alder Rearrangement (RDA)	O-xylene Loss
387.216 (ONC201)	C ₂₄ H ₂₇ N ₄ O ⁺	13	Yes	Yes
190.133 (DP189)	C ₁₁ H ₁₆ N ₃ ⁺	5.5	No	Yes
391.213 (DP390)	C ₂₃ H ₂₇ N ₄ O ₂ ⁺	12.5	Yes	Yes
403.210 (DP402-1)	C ₂₄ H ₂₇ N ₄ O ₂ ⁺	13.5	Yes	Yes
403.210 (DP402-2)	C ₂₄ H ₂₇ N ₄ O ₂ ⁺	13.5	Yes	Yes
407.242 (DP406)	C ₂₄ H ₃₁ N ₄ O ₂ ⁺	12.5	No	Yes
419.219 (DP418)	C ₂₄ H ₂₇ N ₄ O ₃ ⁺	13	No	Yes
421.222 (DP420)	C ₂₄ H ₂₉ N ₄ O ₃ ⁺	12.5	No	No
437.216 (DP436)	C ₂₄ H ₂₉ N ₄ O ₄ ⁺	12.5	Yes	Yes

Indeed, given the presence of several unsaturations and nitrogenous heterocycles on the structure of ONC201, it was to be expected that hydrogen peroxide would interact with these chemical functions leading, initially, to the formation of epoxide and/or N-oxide functions. Thus, the structure of DP402-1 and DP402-2 seems to have supported these hypotheses in the sense that their fragmentation processes corroborate with the fact that DP402-1 would be an N-oxide derivative formed on the amine of the tetrahydropyridine moiety and that DP402-2, co-eluted, would be the result of a localised epoxidation reaction on the former double bond of the tetrahydropyridine moiety carried by ONC201 (Figure 7). This is all the more true since, on the one hand, none of the mass spectra of the degradation products formed in the presence of hydrogen peroxide showed neutral loss of the group at 114 Da, described for ONC201 as coming from the RDA, and on the other hand, that the neutral loss linked to the intact presence of the xylene group was always detected, thus suggesting that the attacks by H₂O₂ systematically targeted the part comprising the tetrahydropyridine linked to the toluene unit of ONC201.

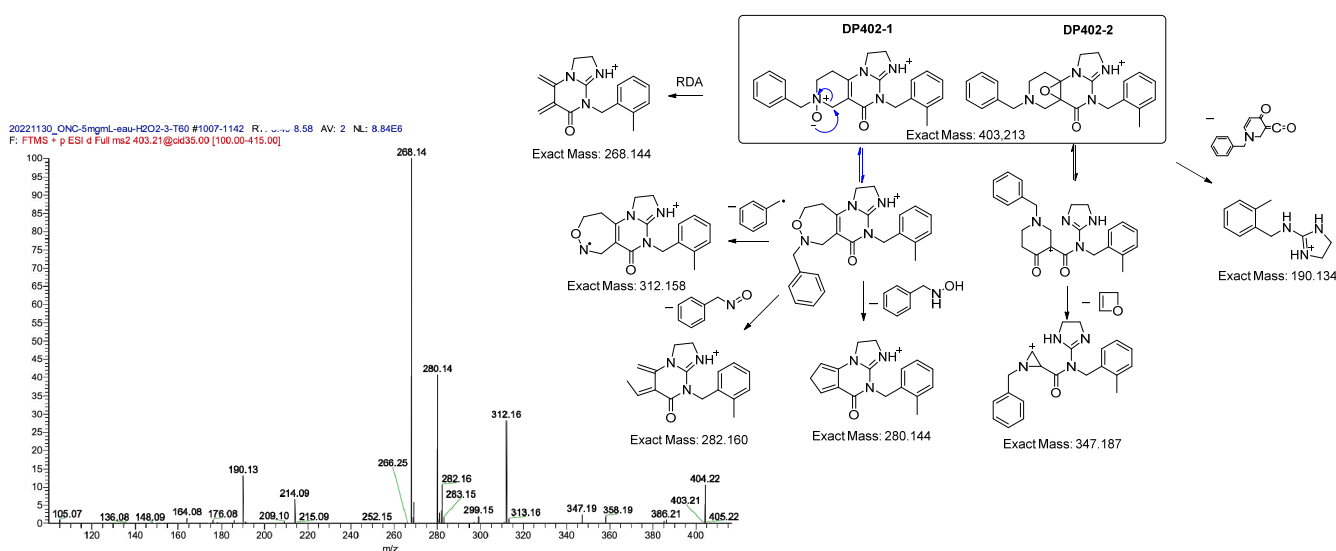


Figure 7. Proposed fragmentation pattern of protonated DP402-1 and DP402-2.

For example, the fragmentation patterns of protonated DP406, DP418, DP420 and DP436 studied in detail go perfectly in this direction as shown in Figures 8–11. More particularly, the behaviours of these molecular ions by collision-induced dissociation suggest in some cases ring opening (DP406 (Figure 8), DP420 (Figure 9)), and in other cases, multiple oxidations involving both the epoxide group and the N-oxide group of the entity tetrahydropyridine DP418 (Figure 10, inset a), DP436 (Figure 10, inset b) and DP 390 (Figure 11).

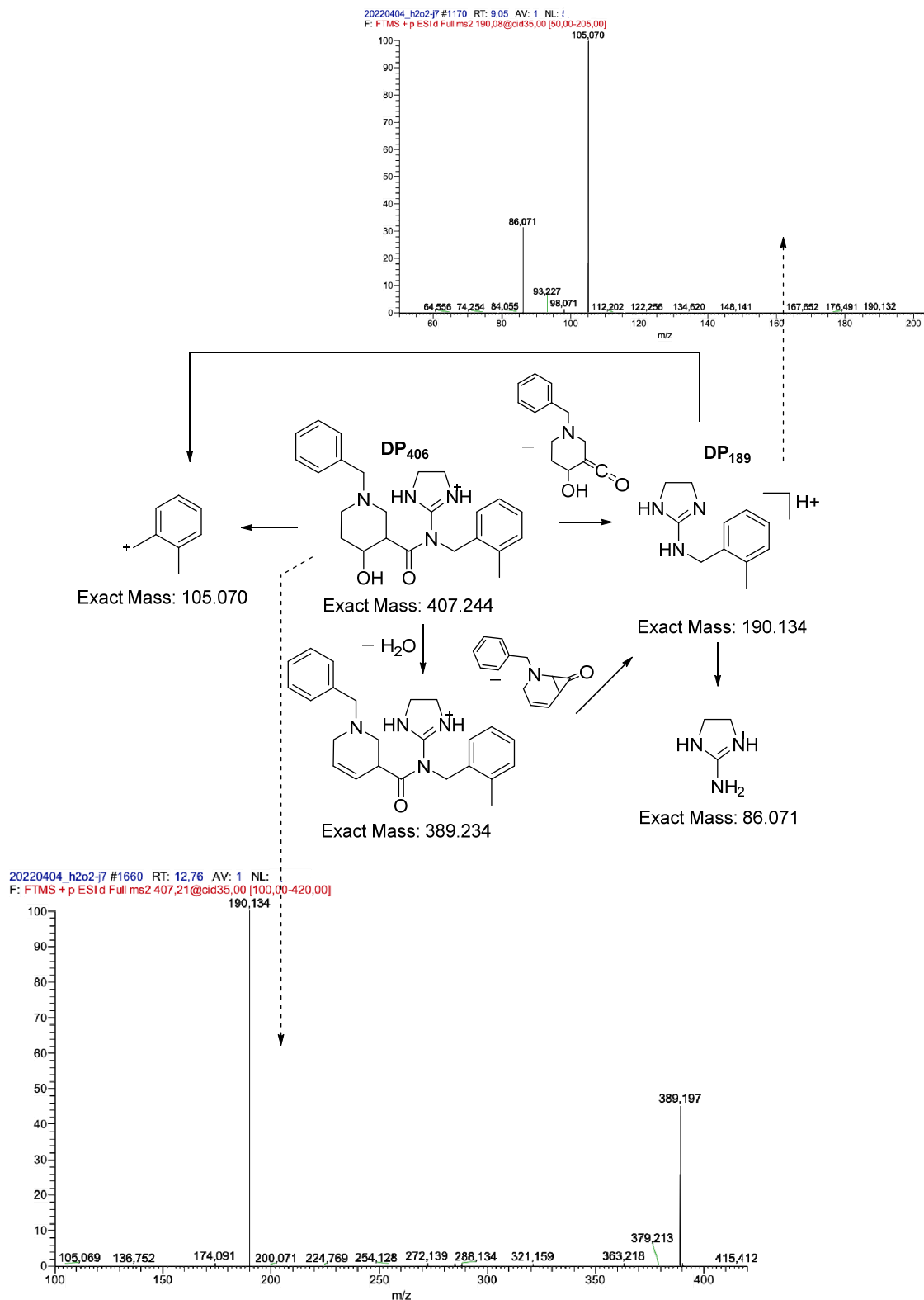


Figure 8. Proposed fragmentation patterns of protonated DP406 and DP189.

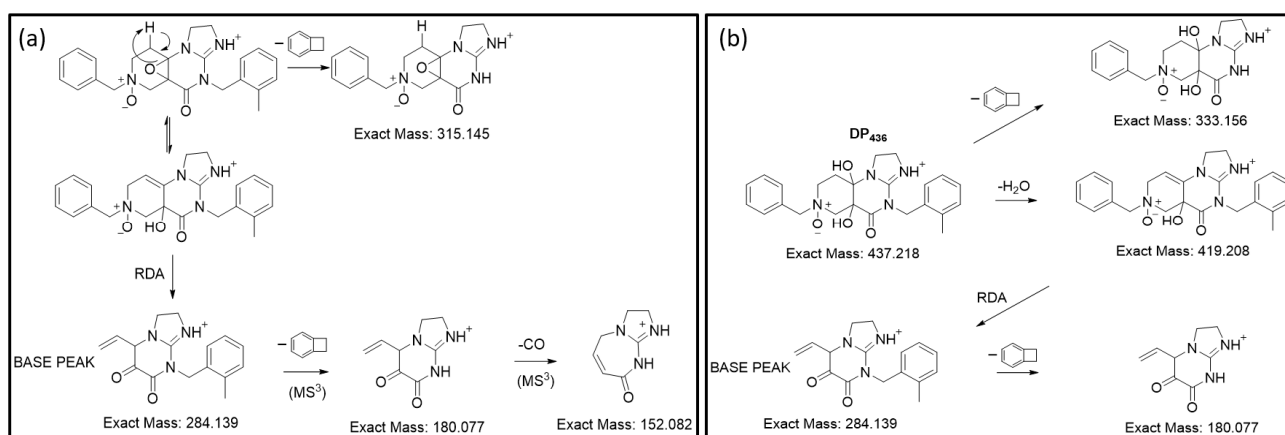


Figure 10. (a) Proposed fragmentation pattern of protonated DP418; (b) proposed fragmentation pattern of protonated DP436.

The degradation product having a lower molecular mass than ONC201, i.e., DP189, is the result of a degradation which is accentuated after the attacks previously mentioned (Figure 11).

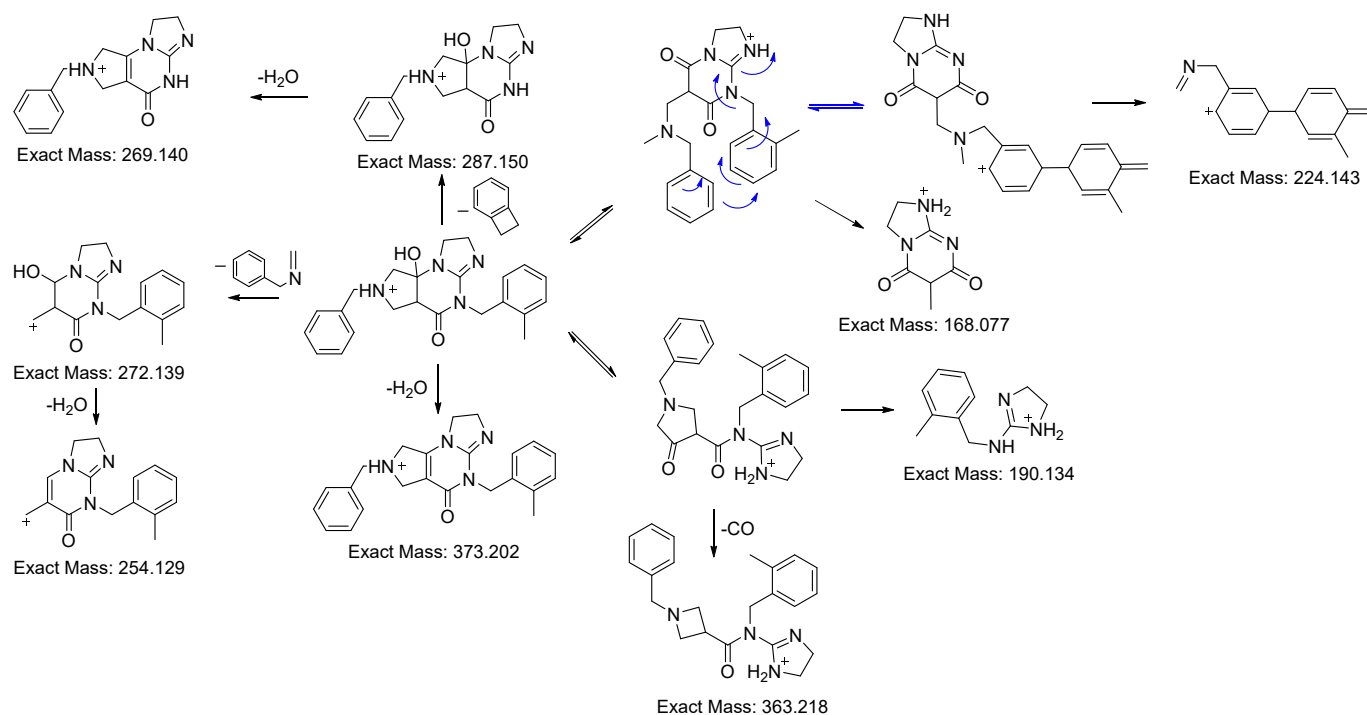


Figure 11. Proposed fragmentation pattern of protonated DP390.

3.3. Continued Preliminary Work on Establishing Specifications for Degradation Products for Release and Stability Control

The structural identification of the DPs set the basis for in silico assessment as per ICH M7, from which a specification for the DPs in the drug product can be proposed.

To comply with guidance of ICH M7 [22], two computational approaches were used to assess the mutagenic potential of the tentatively identified DPs. This process allowed the tested DPs to be compared to ONC201 in order to provisionally establish their acceptable limits [35]. This comparison made it possible to classify these DPs according to risk, know-

ing that contradictory results between the two computational approaches automatically favour the one that identifies the risk (Table S1):

- Knowing that ONC201 is already an anti-cancer agent classified as a mutagen, according to the rule-based Toxtree software, if DPs show warning structures unrelated to the structure of ONC201, they should be controlled below a threshold of toxicological concern or a bacterial mutagenicity assessment should be performed (class 3);
- If the DPs have warning structures already present on the ONC201 structure (class 4) or simply do not have any (class 5), they are in either case considered mutagenic.

The rule-based software considered the hex-1-en-3-one group in the ONC201 structure as an alert. This is therefore also the case for DP 390, DP402-1, DP418, DP398 1-3. For these, in the stability test, we will not consider them as specified impurities to be tested. If they are detected at a threshold of less than 0.1%, we will ignore them. If they appear individually at a relative value exceeding a provisionally defined threshold of 0.15%, we will monitor them over time, taking this result as an out-of-trend to be evaluated.

However, not all provisionally identified DPs are so favourable. ONC201 isomer, DP402-2, DP292, DP436, DP418 1-2, and DP384 1-2 are indeed in class 3. This is why, following this work, we must plan to carry out Ames tests on samples that have been degraded under the conditions in which we were able to detect their appearance.

4. Conclusions

Stress testing and LC-MS-HRMS studies have enabled us to tentatively identify the main degradation products of ONC201. The structural changes comprised alterations of the imidazole, the tetrahydropyridine and piperidine rings as well as displacements of benzyl and *o*-xylene rings. Further experimental and theoretical studies will be carried out to explain the mechanisms involved in the degradation process and to determine measures to reduce the formation of the degradation products.

The structures of the degradation products set the basis for preliminary risk assessment, using *in silico* assessment, where it was shown that some degradation products raised some toxicological concerns. These results will pave the way to design an appropriate control strategy, comprising a specific stability-indicating method to follow up these potentially toxic degradation products and verify that the other degradation products do not exceed the qualification thresholds.

Supplementary Materials: The following supporting information can be downloaded at: <https://www.mdpi.com/article/10.3390/chemosensors11050294/s1>, Table S1: relative retention time and results of the *in silico* assessment for the identified compounds; Figure S1: degradation kinetics of ONC201. Inset (a) under photolytic conditions. Inset (b) under oxidising conditions; Figure S2: LC-MS-HRMS mass spectra of protonated ONC201; Figure S3: LC-MS-HRMS mass spectra of protonated DP190; Figure S4: LC-HRMS² mass spectra of protonated DP292; Figure S5: LC-MS-HRMS mass spectra of protonated DP382; Figure S6: LC-HRMS² mass spectra of protonated DP385; Figure S7: LC-MS-HRMS mass spectra of protonated DP398; Figure S8: LC-MS-HRMS mass spectra of protonated DP418; Figure S9: LC-MS-HRMS mass spectra of protonated DP390; Figure S10: LC-MS-HRMS mass spectra of protonated DP402; Figure S11: LC-MS-HRMS mass spectra of protonated DP406; Figure S12: LC-MS-HRMS mass spectra of protonated DP418; Figure S13: LC-MS-HRMS mass spectra of protonated DP420.

Author Contributions: Conceptualization, M.A., A.R., J.G., P.-H.S. and B.D.; data curation, M.V., T.S.E.B. and A.S.; formal analysis, M.A., P.-H.S. and B.D.; funding acquisition, M.P. and A.R.; investigation, M.A., M.V., T.S.E.B., L.D., A.S., V.V. and P.-H.S.; methodology, M.A., V.V., M.P., P.-H.S. and B.D.; resources, M.P. and A.R.; supervision, M.A., P.-H.S. and B.D.; visualization, M.A., M.V., T.S.E.B. and L.D.; writing—original draft, M.A., P.-H.S. and B.D.; writing—review and editing, L.D., A.S., V.V., M.P., A.R. and J.G. All authors have read and agreed to the published version of the manuscript.

Funding: This research received no external funding.

Institutional Review Board Statement: Not applicable.

Informed Consent Statement: Not applicable.

Data Availability Statement: Not applicable.

Conflicts of Interest: The authors declare no conflict of interest.

References

1. Clinicaltrials.gov. Chimerix Oral ONC201 in Recurrent Glioblastoma, H3 K27M-Mutant Glioma, and Diffuse Midline Glioma. Available online: <https://clinicaltrials.gov/ct2/show/NCT02525692> (accessed on 1 March 2023).
2. Clinicaltrials.gov. Chimerix ONC201 for the Treatment of Newly Diagnosed H3 K27M-Mutant Diffuse Glioma Following Completion of Radiotherapy: A Randomized, Double-Blind, Placebo-Controlled, Multicenter Study. Available online: <https://clinicaltrials.gov/ct2/show/NCT05580562> (accessed on 1 March 2023).
3. Clinicaltrials.gov. Winer, I. Phase II Study of ONC201 Plus Weekly Paclitaxel in Patients with Platinum-Resistant Refractory or Recurrent Epithelial Ovarian, Fallopian Tube, or Primary Peritoneal Cancer. Available online: <https://clinicaltrials.gov/ct2/show/NCT04055649> (accessed on 1 March 2023).
4. Clinicaltrials.gov. National Cancer Institute (NCI) Phase 1 Trial of ONC201 for Chemoprevention of Colorectal Cancer. Available online: <https://clinicaltrials.gov/ct2/show/NCT05630794> (accessed on 1 March 2023).
5. Bonner, E.R.; Waszak, S.M.; Grotzer, M.A.; Mueller, S.; Nazarian, J. Mechanisms of imipridones in targeting mitochondrial metabolism in cancer cells. *Neuro. Oncol.* **2021**, *23*, 542–556. [[CrossRef](#)] [[PubMed](#)]
6. Allen, J.E.; Crowder, R.; El-Deiry, W.S. First-In-Class Small Molecule ONC201 Induces DR5 and Cell Death in Tumor but Not Normal Cells to Provide a Wide Therapeutic Index as an Anti-Cancer Agent. *PLoS ONE* **2015**, *10*, e0143082. [[CrossRef](#)] [[PubMed](#)]
7. Clinicaltrials.gov. Gustave Roussy, Cancer Campus, Grand Paris Biological Medicine for Diffuse Intrinsic Pontine Glioma (DIPG) Eradication. Available online: <https://clinicaltrials.gov/ct2/show/NCT05476939> (accessed on 1 March 2023).
8. Kurmi, M.; Sahu, A.; Ladumor, M.K.; Kumar Bansal, A.; Singh, S. Stability behaviour of antiretroviral drugs and their combinations. 9: Identification of incompatible excipients. *J. Pharm. Biomed. Anal.* **2019**, *166*, 174–182. [[CrossRef](#)] [[PubMed](#)]
9. Kurmi, M.; Sahu, A.; Balhara, A.; Singh, I.P.; Kulkarni, S.; Singh, N.K.; Garg, P.; Singh, S. Stability behaviour of antiretroviral drugs and their combinations. 11: Characterization of interaction products of zidovudine and efavirenz, and evaluation of their anti HIV-1 activity, and physiochemical and ADMET properties. *J. Pharm. Biomed. Anal.* **2020**, *178*, 112911. [[CrossRef](#)] [[PubMed](#)]
10. Singh, D.K.; Sahu, A.; Wani, A.A.; Bharatam, P.V.; Kotimoole, C.N.; Batkulwar, K.B.; Deshpande, A.Y.; Giri, S.; Singh, S. Stability behaviour of antiretroviral drugs and their combinations. 10: LC-HRMS, LC-MSn, LC-NMR and NMR characterization of fosamprenavir degradation products and in silico determination of their ADMET properties. *Eur. J. Pharm. Biopharm.* **2019**, *142*, 165–178. [[CrossRef](#)]
11. Rajput, N.; Soni, F.; Sahu, A.K.; Jadav, T.; Sharma, S.; Sengupta, P. Degradation kinetics and characterization of major degradants of binimetinib employing liquid chromatography-high resolution mass spectrometry. *J. Pharm. Biomed. Anal.* **2022**, *215*, 114753. [[CrossRef](#)]
12. Chavan, B.B.; Sawant, V.; Borkar, R.M.; Ragampeta, S.; Talluri, M.V.N.K. Isolation and structural characterization of degradation products of afatinib dimaleate by LC-Q-TOF/MS/MS and NMR: Cytotoxicity evaluation of afatinib and isolated degradation products. *J. Pharm. Biomed. Anal.* **2019**, *166*, 139–146. [[CrossRef](#)]
13. Golla, V.M.; Kushwah, B.S.; Dhiman, V.; Velip, L.; Samanthula, G. LC-HRMS and NMR studies for characterization of forced degradation impurities of ponatinib, a tyrosine kinase inhibitor, insights into in-silico degradation and toxicity profiles. *J. Pharm. Biomed. Anal.* **2023**, *227*, 115280. [[CrossRef](#)]
14. Secretan, P.-H.; Annereau, M.; Kini-Matondo, W.; Prost, B.; Prudhomme, J.; Bourmane, L.; Paul, M.; Yagoubi, N.; Sadou-Yayé, H.; Do, B. Unequal Behaviour between Hydrolysable Functions of Nirmatrelvir under Stress Conditions: Structural and Theoretical Approaches in Support of Preformulation Studies. *Pharmaceutics* **2022**, *14*, 1720. [[CrossRef](#)]
15. Bouchema, T.S.; Annereau, M.; Vieillard, V.; Boquet, R.; Coelho, G.A.; Castelli, F.; Solgadi, A.; Paul, M.; Yagoubi, N.; Secretan, P.-H.; et al. Identification of the Major Degradation Pathways of Selumetinib. *Pharmaceutics* **2022**, *14*, 2651. [[CrossRef](#)]
16. da Silva, J.W.V.; Ribeiro, J.I.; de Souza, L.X.; da Silva Aquino, K.A.; Kishishita, J.; Sobrinho, J.L.S.; Leal, L.B.; de Castro, W.V.; de Santana, D.P.; Bedor, D.C.G. Development of the stability-indicating method, structural elucidation of new photodegradation products from terconazole by LC-MS TOF, and in vitro toxicity. *J. Pharm. Biomed. Anal.* **2022**, *216*, 114794. [[CrossRef](#)] [[PubMed](#)]
17. EMA ICH Q1A (R2) Stability Testing of New Drug Substances and Products-Scientific Guideline. Available online: <https://www.ema.europa.eu/en/ich-q1a-r2-stability-testing-new-drug-substances-drug-products-scientific-guideline> (accessed on 29 March 2023).
18. Baertschi, S.W.; Alsante, K.M.; Reed, R.A. *Pharmaceutical Stress Testing: Predicting Drug Degradation*, 2nd ed.; CRC Press: Boca Raton, FL, USA, 2016; ISBN 978-0-429-13608-5.
19. Blessy, M.; Patel, R.D.; Prajapati, P.N.; Agrawal, Y.K. Development of forced degradation and stability indicating studies of drugs—A review. *J. Pharm. Anal.* **2014**, *4*, 159–165. [[CrossRef](#)] [[PubMed](#)]
20. Liu, Y.; Romijn, E.P.; Verniest, G.; Laukens, K.; De Vijlder, T. Mass spectrometry-based structure elucidation of small molecule impurities and degradation products in pharmaceutical development. *TrAC Trends Anal. Chem.* **2019**, *121*, 115686. [[CrossRef](#)]
21. EMA ICH Q1B Photostability Testing of New Active Substances and Medicinal Products-Scientific Guideline. Available online: <https://www.ema.europa.eu/en/ich-q1b-photostability-testing-new-active-substances-medicinal-products-scientific-guideline> (accessed on 29 March 2023).

22. EMA ICH M7 Assessment and Control of DNA Reactive (Mutagenic) Impurities in Pharmaceuticals to Limit Potential Carcinogenic Risk-Scientific Guideline. Available online: <https://www.ema.europa.eu/en/ich-m7-assessment-control-dna-reactive-mutagenic-impurities-pharmaceuticals-limit-potential> (accessed on 28 March 2023).
23. Patlewicz, G.; Jeliakova, N.; Safford, R.J.; Worth, A.P.; Aleksiev, B. An evaluation of the implementation of the Cramer classification scheme in the Toxtree software. *SAR QSAR Environ. Res.* **2008**, *19*, 495–524. [[CrossRef](#)] [[PubMed](#)]
24. Toropov, A.A.; Toropova, A.P.; Raska, I.; Leszczynska, D.; Leszczynski, J. Comprehension of drug toxicity: Software and databases. *Comput. Biol. Med.* **2014**, *45*, 20–25. [[CrossRef](#)] [[PubMed](#)]
25. EMA ICH Q3A (R2) Impurities in New Drug Substances-Scientific Guideline. Available online: <https://www.ema.europa.eu/en/ich-q3a-r2-impurities-new-drug-substances-scientific-guideline> (accessed on 28 March 2023).
26. EMA ICH Q3B (R2) Impurities in New Drug Products-Scientific Guideline. Available online: <https://www.ema.europa.eu/en/ich-q3b-r2-impurities-new-drug-products-scientific-guideline> (accessed on 28 March 2023).
27. Śliwka-Kaszyńska, M.; Anusiewicz, I.; Skurski, P. The Mechanism of a Retro-Diels–Alder Fragmentation of Luteolin: Theoretical Studies Supported by Electrospray Ionization Tandem Mass Spectrometry Results. *Molecules* **2022**, *27*, 1032. [[CrossRef](#)] [[PubMed](#)]
28. Cuyckens, F.; Claeys, M. Mass spectrometry in the structural analysis of flavonoids. *J. Mass Spectrom.* **2004**, *39*, 1–15. [[CrossRef](#)]
29. Wagner, J.; Kline, C.L.; Pottorf, R.S.; Nallaganchu, B.R.; Olson, G.L.; Dicker, D.T.; Allen, J.E.; El-Deiry, W.S. The angular structure of ONC201, a TRAIL pathway-inducing compound, determines its potent anti-cancer activity. *Oncotarget* **2014**, *5*, 12728–12737. [[CrossRef](#)]
30. Wasserman, H.H.; Stiller, K.; Floyd, M.B. The reactions of heterocyclic systems with singlet oxygen. Photosensitized oxygenation of imidazoles. *Tetrahedron Lett.* **1968**, *9*, 3277–3280. [[CrossRef](#)]
31. Huang, Y.; Su, B.-N.; Marshall, J.; Miller, S.A. Forced Oxidative Degradation Pathways of the Imidazole Moiety of Daclatasvir. *J. Pharm. Sci.* **2019**, *108*, 3312–3318. [[CrossRef](#)]
32. Seburg, R.A.; Ballard, J.M.; Hwang, T.-L.; Sullivan, C.M. Photosensitized degradation of losartan potassium in an extemporaneous suspension formulation. *J. Pharm. Biomed. Anal.* **2006**, *42*, 411–422. [[CrossRef](#)] [[PubMed](#)]
33. Pan, H. A non-covalent dimer formed in electrospray ionisation mass spectrometry behaving as a precursor for fragmentations: Non-covalent dimer as a precursor for ESI-MS fragmentations. *Rapid Commun. Mass Spectrom.* **2008**, *22*, 3555–3560. [[CrossRef](#)] [[PubMed](#)]
34. Wan, D.; Yang, H.; Yan, C.; Song, F.; Liu, Z.; Liu, S. Differentiation of glucose-containing disaccharides isomers by fragmentation of the deprotonated non-covalent dimers using negative electrospray ionization tandem mass spectrometry. *Talanta* **2013**, *115*, 870–875. [[CrossRef](#)] [[PubMed](#)]
35. Müller, L.; Mauthe, R.J.; Riley, C.M.; Andino, M.M.; Antonis, D.D.; Beels, C.; DeGeorge, J.; De Knaep, A.G.M.; Ellison, D.; Fagerland, J.A.; et al. A rationale for determining, testing, and controlling specific impurities in pharmaceuticals that possess potential for genotoxicity. *Regul. Toxicol. Pharmacol.* **2006**, *44*, 198–211. [[CrossRef](#)]

Disclaimer/Publisher’s Note: The statements, opinions and data contained in all publications are solely those of the individual author(s) and contributor(s) and not of MDPI and/or the editor(s). MDPI and/or the editor(s) disclaim responsibility for any injury to people or property resulting from any ideas, methods, instructions or products referred to in the content.